DYNAMICS OF WEAKLY RELATIVISTIC ELECTROMAGNETIC SOLITONS IN LASER PLASMAS

Lj. Hadžievski[1], A. Mančić[2], M. M. Škorić[3]

*[1]Vinča Institute of Nuclear Sciences,
P. O. Box 522, 11001 Belgrade, Serbia
[2]Department of Physics, Faculty of Sciences and Mathematics,
University of Niš, P. O. B. 224, 18001 Niš, Serbia
[3]National Institute for Fusion Science, Toki, 509-5292, Japan*

Abstract. Dynamical features of one-dimensional electromagnetic solitons formed in a relativistic interaction of a linearly polarized laser light with underdense cold plasma are investigated. The relativistic Lorentz force in an intense laser light pushes electrons into longitudinal motion generating coupled longitudinal-transverse waves. In a weakly relativistic approximation these modes are well described by the generalized nonlinear Schrödinger type of equation, with two extra nonlocal terms. Here, an original analytical solution for a *moving* EM soliton is derived in an implicit form. For an isolated soliton, our analysis shows that the motion down-shifts the soliton eigen-frequency and decreases its amplitude. The effect of the soliton velocity on the stability, is analytically predicted and checked numerically. Results show an enhanced stability in comparison with the standing soliton case. Rich dynamics with examples of (un)stable soliton propagation and breathers creation and formation of unstable structures of cusp type is exposed numerically. The soliton stability is a base for the understanding a complex soliton-pair interaction; which critically depends on solitons amplitude, velocity and a mutual phase relation. Simulations of two interacting EM solitons show a critical dependence on the solitons amplitude, velocity and mutual phase; resulting in either elastic collisions or a break up of the soliton pair.

1. INTRODUCTION

The propagation of intense laser radiation into plasmas has attracted considerable attention in the past. Recently, the interest for this problem is renewed mainly due to two prospective applications: development of the fast ignition concept

in inertial fusion and x-ray lasers. Currently, available laser intensity is as high as $10^{21}\,\mathrm{W/cm}^2$ at a focus, with tendency to reach soon $10^{23}\,\mathrm{W/cm}^2$. These intensities are well above the regime where, in the laser plasma interactions, the electrons are forced into motion with relativistic velocities. This strongly affects the dynamics of the laser pulse propagation and with combination of the nonlinear effects induces a large number of nonlinear relativistic phenomena. One of the most interesting phenomena is creation of the relativistic electromagnetic (EM) solitons. Relativistic EM solitons are localized EM structures self-trapped by a locally modified plasma refractive index due to the relativistic electron mass increase and the electron density drop in the ponderomotive force of an intense laser light. These solitons, generated behind the front of the laser pulse are composed of nonlinear, spatially localized low-frequency EM fields with a group velocity close to zero. A large part of the laser pulse energy can be trapped inside these relativistic solitons, creating a significant channel for laser beam energy conversion. This is a known problem in plasma physics which has been studied widely in the past [1-8] but it has recently attracted fresh attention. The relativistic EM solitons in an idealized case of circular polarization were extensively investigated, analytically within the one-dimensional (1D) fully relativistic hydrodynamics model and by PIC (particle-in-cell) simulations [1, 9]. Recently, relativistic EM solitons in electron-ion plasmas have been studied in detail, analytically [9-14], numerically by fluid simulations [15] and by multi-dimensional PIC simulations [7,16-20]. On the other hand, a physically more realistic, but also a more complex case of relativistic EM solitons with a linear polarization, was studied in a weak amplitude limit by some of these authors [20, 21]. Generally taken, the research on solitons has been receiving much attention because of their fundamental importance in nonlinear science [4], as well as being considered to be the essential component of plasma turbulence [13].

In this paper, we treat a case of a linearly polarized intense laser light. In laser-plasma interactions, relativistic Lorentz force sets electrons into motion, generating coupled longitudinal-transverse wave modes. These modes in the framework of one-dimensional weakly relativistic cold plasma approximation can be well described by a single dynamical equation of the generalized nonlinear Schrödinger type[21], with two extra nonlocal (derivative) terms. A new analytical solution for the one-dimensional *moving* EM soliton case is calculated in the implicit form and verified numerically. The soliton existence and its stability properties depending on the soliton velocity and self-frequency shift are studied in detail, by using analytically calculated conserved quantities: photon number (P) and Hamiltonian (H). The results are compared to the standing (non-moving) relativistic EM solitons case [21]. Finally, numerical simulations of the model equation were performed to check the analytical results and study soliton dynamics influenced by small perturbations. A good agreement with our analytical results is found. The results of the soliton stability analysis are base for the understanding a complex soliton-pair interaction, which critically depends on solitons amplitude, velocity and a mutual phase relation. Simulations of two interacting EM solitons show a critical dependence on the solitons amplitude, velocity and mutual phase; resulting in either elastic collisions or a break up of the soliton pair.

2. DYNAMICAL EQUATIONS

We consider a long intense laser pulse propagating through cold collisionless plasma with fixed ions and start with writing the fully relativistic one-dimensional model. The nonlinear EM wave equation, continuity equation and electron momentum equation, in the Coulomb gauge, read:

$$\left(\frac{\partial^2}{\partial t^2} - c^2 \frac{\partial^2}{\partial x^2}\right) a = -\frac{\omega_p^2}{n_0} \frac{n}{\gamma} a \tag{1}$$

$$\frac{\partial n}{\partial t} + \frac{\partial}{\partial x}\left(\frac{np}{m\gamma}\right) = 0 \tag{2}$$

$$\frac{\partial p}{\partial t} = -eE_{\parallel} - mc^2 \frac{\partial \gamma}{\partial x} \tag{3}$$

where $a = eA/mc^2$ is normalized vector potential in the y direction, n is the electron density, p is the electron momentum in the x direction, $\gamma = (1 + a^2 + p^2/m^2c^2)^{1/2}$, $E_{\parallel}$ is the longitudinal electric field, n_0 is the unperturbed electron density, and $\omega_p = (4\pi e^2 n_0/m)^{1/2}$ is the background electron plasma frequency.

In a weakly relativistic limit for $|a| << 1$ and $|\delta n| << 1$, introducing the normalized perturbed electron density $\delta n = (n - n_0)/n_0$ and dimensionless variables $x \to (c\omega_p^{-1})x$ and $t \to (\omega_p^{-1})t$, the wave equation for the vector potential envelope A ($a \sim A \cdot e^{-it} + cc$) is obtained, as (details are given in Ref. 21):

$$i\frac{\partial A}{\partial t} + \frac{1}{2}A_{xx} + \frac{3}{16}|A|^2 A - \frac{1}{8}(|A|^2)_{xx} A + \frac{1}{48}(A^2)_{xx} A^* = 0 \tag{4}$$

Equation (4) has a form of a generalized nonlinear Schrödinger (GNLS) equation with two extra nonlocal (derivative) nonlinear terms. We can readily derive three conserved quantities: photon number P and Hamiltonian H and momentum M:

$$P = \int |A|^2 \, dx,$$

$$H = \frac{1}{2}\int \left\{|A_x|^2 - \frac{3}{16}|A|^4 - \frac{1}{8}[(|A|^2)_x]^2 + \frac{1}{12}|A|^2 |A_x|^2\right\} dx$$

$$\tag{5}$$

$$M = i\int \left(A \cdot A_x^* - A^* \cdot A_x\right) dx$$

103

We look for a localized stationary solution of (4), in a form of a moving soliton:

$$A = \rho(u)\exp[i\theta(u) + i\lambda^2 t] \tag{6}$$

where, $u = x - vt$, and v is the soliton velocity. Introducing the ansatz (6) in the equation (4), we obtain two equations for the soliton phase and amplitude, respectively:

$$\theta_{uu}\rho(1 + \frac{1}{12}\rho^2) + \theta_u\rho_u(2 + \frac{1}{3}\rho^2) - 2v\rho_u = 0 \tag{7a}$$

$$\rho_{uu} - \frac{\frac{5}{12}\rho}{1 - \frac{5}{12}\rho^2}\rho_u{}^2 = \frac{\left(\frac{\theta_u{}^2}{6} - \frac{3}{8}\right)\rho^3 + \left(2\lambda^2 - 2v\theta_u + \theta_u{}^2\right)\rho}{\left(1 - \frac{5}{12}\rho^2\right)} \tag{7b}$$

Under vanishing (localized) boundary conditions $\rho(u), \rho(u)_u, \rho(u)_{uu} \to 0$ for $u \to \pm\infty$, the first integration of (7a) approximately gives $\theta_u(u) = v$, while the first integration of (7b) gives:

$$(\rho_u)^2 = \frac{2\lambda^2 - v^2 - \left(\frac{3}{16} - \frac{v^2}{12}\right)\rho^2}{1 - \frac{5}{12}\rho^2}\rho^2 \tag{8}$$

Additional integration of (8) yields a moving soliton solution in an implicit form

104

$$\pm u = \frac{1}{2\sqrt{2\lambda^2 - v^2}} \ln \frac{\sqrt{1 - \frac{\rho^2}{\rho_0^2}} + \sqrt{1 - \frac{5}{12}\rho^2}}{\left|\sqrt{1 - \frac{\rho^2}{\rho_0^2}} - \sqrt{1 - \frac{5}{12}\rho^2}\right|}$$

$$-\frac{1}{\sqrt{\frac{9}{20} - \frac{v^2}{5}}} \ln \frac{\sqrt{1 - \frac{5}{12}\rho^2} + \sqrt{\frac{5}{12}\rho_0^2 - \frac{5}{12}\rho^2}}{\sqrt{\left|1 - \frac{5}{12}\rho_0^2\right|}} \tag{9}$$

where $\rho_0^{\ 2} = \dfrac{2\lambda^2 - v^2}{3/16 - v^2/12}$ is the maximum amplitude of the linearly polarized moving EM soliton with the self-frequency $\Lambda = \lambda^2 - v^2$. For a zero soliton velocity, $v = 0$, the above solution readily coincides with the standing soliton result of the GNLS equation (4), given by some of these authors [21]. The equation (9) imposes the constraint on the maximum possible soliton amplitude, as $\rho_c < \sqrt{12/5} \approx 1.55$. For $\rho_0 << 1.55$ the soliton profile (9) is the secant hyperbolic, alike the soliton solution of the standard cubic NLS equation. When ρ_0 increases and approaches the value of $\rho_c \approx 1.55$, the original NLS soliton profile steepens and transits toward the pointed, cusp type of a profile.

In order to check the validity of the analytical solution (9), the stationary equations (7a,b) are numerically solved with the vanishing boundary conditions $\rho(u), \rho(u)_u, \rho(u)_{uu} \to 0$ when $u \to \pm\infty$. Numerical results are in a good agreement with the analytical solution for the amplitude (9) and phase $\theta(u)$ (Fig. 1). The only noticeable difference is in the phase $\theta(u)$ (analytical approximation).
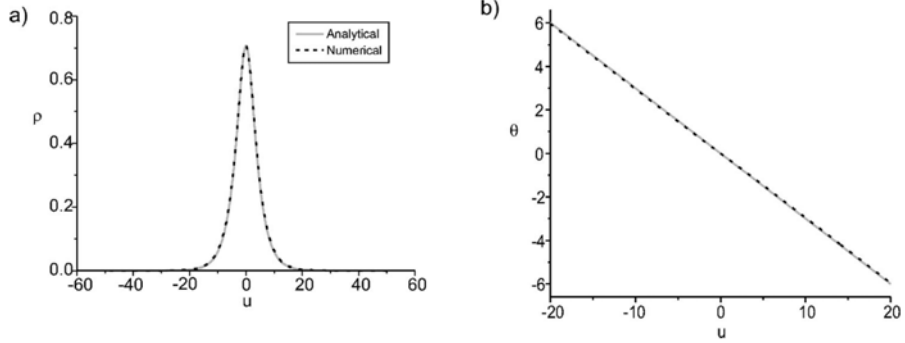
Fig. 1. Example of the EM soliton amplitude profile (a) and phase (b) calculated analytically and numerically for $v=0.4$ and $\lambda=0.3$.

The photon number $P(\lambda, v)$ for the soliton (9), can be calculated explicitly, as:

$$P_0(\lambda, v) = \frac{1}{\sqrt{3/16 - v^2/12}} \left[\rho_0 + \sqrt{\frac{3}{5}} \left(1 - 5\rho_0^2/12\right) \ln \frac{1 + \rho_0 \sqrt{5/12}}{\left|1 - \rho_0 \sqrt{5/12}\right|} \right] \quad (10)$$

When the soliton velocity is zero, expression (10) agrees with the standing soliton solution, obtained earlier [21].

Furthermore, with the ansatz (6), explicit contribution of the velocity dependent - "kinetic" terms in the Hamiltonian (5) is singled out, by:

$$H = \int \left[\left(1 - \frac{5}{12}\rho^2\right)\rho_u + \frac{v^2 \rho^2}{\rho_u} - \left(\frac{3}{16} - \frac{v^2}{12}\right)\frac{\rho^4}{\rho_u} \right] d\rho \quad (11)$$

Substitution of (9) into (11) enables us, after rather cumbersome integration, to obtain the explicit analytical expression for the Hamiltonian in a form:

106

$$H_0 = \frac{3}{200} \frac{40\lambda^2 - 64v^2 + 9}{\sqrt{2\lambda^2 - v^2}} \left(1 - \frac{12}{5\rho_0^2}\right)\left(\frac{5\rho_0^2}{12}\right)^{3/2} \ln \frac{1 + \sqrt{\frac{12}{5\rho_0^2}}}{\left|1 - \sqrt{\frac{12}{5\rho_0^2}}\right|}$$

$$+ \frac{\sqrt{2\lambda^2 - v^2}}{4}\left(\frac{12}{5} + \frac{3v^2 - 2\lambda^2}{\frac{3}{16} - \frac{v^2}{12}}\right) \tag{12}$$

3. STABILITY ANALYSIS

In order to check the stability of the moving soliton, we use the renown Vakhitov-Kolokolov stability criterion [2], according to which, solitons are stable with respect to longitudinal perturbations, if:

$$\frac{dP_o}{d\lambda^2} > 0, \tag{13}$$

where, P_0 is the soliton photon number defined by (5). The function $P_0(\lambda)$, given by the expression (10), is shown in Fig. 2, for several values of soliton velocity.
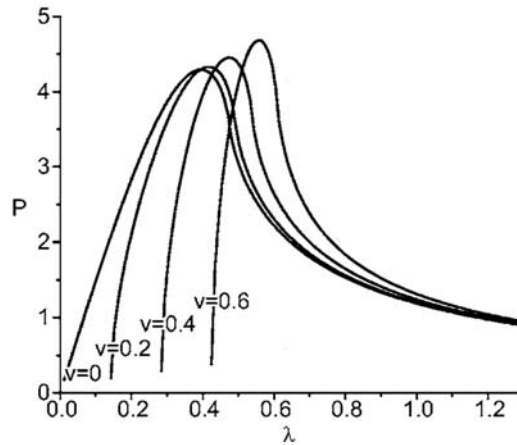
Fig. 2. Photon number $P_0(\lambda)$ shown for different soliton velocities.

According to the condition (13), moving EM solitons turn out to be stable in the region $\lambda < \lambda_s$, where the instability threshold, λ_s corresponds to the maximum value of P_0 for a given velocity (Fig. 2). Therefore, we can conclude that small amplitude linearly polarized moving solitons within the weakly relativistic model are stable. The increase of the soliton velocity shifts the instability threshold λ_s toward larger values leading to the enhanced stability in comparison to the standing soliton case.

The stability criterion for solitons can be alternatively formulated in terms of Hamiltonian and photon number interrelation, following the analysis given in Ref. 22. According to Ref. 22, the concavity of the *H-P* curves is related to the stability of the solitons: concave downwards implies stability, while concave upwards corresponds to instability. This is illustrated in Fig. 3, where *H-P* curves for different soliton velocities are plotted. There are two branches for each soliton velocity: the upper, unstable and the lower, stable branch. The turning point (maximum value of *P*) on each *H-P* curve coincides with the maximum value of P_0 on $P_0(\lambda)$ diagram (Fig.2) for corresponding soliton velocity and produces the same instability threshold values λ_s. The numerically calculated curves $P_0(\lambda)$ and $H_0(P_0)$ are in a good agreement with the analytical results.
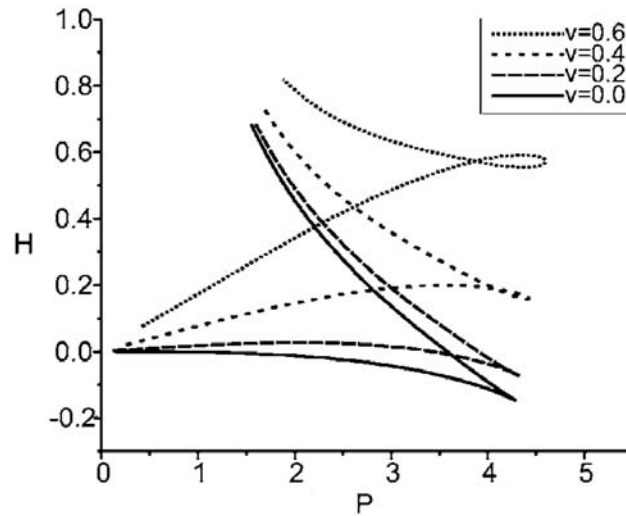
Fig. 3. Hamiltonian versus photon number for different soliton velocities. The lower branches are stable.

Considering the Vakhitov-Kolokolov stability criterion and the constraints on parameters λ, v in the analytical soliton solution (9), we can further expose different regions of the soliton existence and stability. The limits on the parameters λ, v:

$$1 - 5\rho(\lambda, v)^2 / 12 > 0, \quad 2\lambda^2 - v^2 > 0 \tag{14}$$

together with the soliton stability condition $dP / d\lambda^2 > 0$, define the regions of the soliton existence and stability in (λ, v) space. These regions are shown in Fig. 4.

Above the curve (*a*) no analytical soliton solution exists. However, numerically we can find the stationary soliton solution. Discrepancy in numerical and analytical results in this region is attributed to small initial differences in the phase $\theta(u)$ between the approximate analytical and numerical solutions. Below the curve (c), there are no localized solutions, neither analytical nor numerical. The area of the soliton existence is separated by curve (b). Above the curve (b) is the region where $dP_0 / d\lambda^2 < 0$, resulting in the existence of the unstable solitons. The stable soliton solutions are possible just between curves (b) and (c), where the stability condition $dP_0 / d\lambda^2 > 0$, is satisfied.
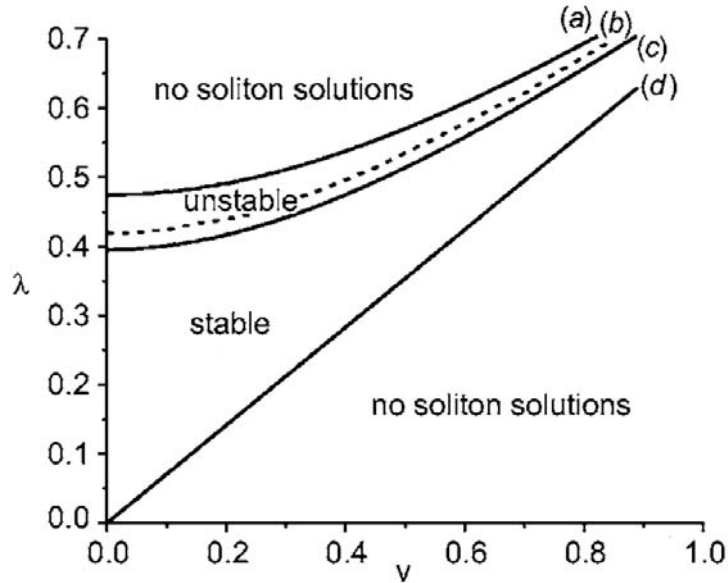
Fig. 4. Soliton existence and stability in different regions of (λ, v) parameter space. Curve (a) 1-5ρ(λ,v)2/12=0, curve (b) dP/dλ2=0 and curve (c) 2λ2-v2=0.

4. SIMULATION RESULTS

In order to check analytical results and our predictions concerning the moving relativistic EM soliton properties and the velocity effect on its existence and stability, we have performed a set of direct numerical simulations of the nonlinear model GNLS equation (4). The split-step Fourier method [23], originally developed for the NLS equation, is implemented in our numerical algorithm.

Numerical results prove that initially launched moving solitons (9), with parameters inside the stability region, bordered with the curves (b) and (c) in Fig. 4., remain stable. The initially unstable solitons with parameters in the region bordered with curves (a) and (b) in Fig. 4. exhibit a slow oscillatory relaxation toward the corresponding stable solitons with the same photon number.

The analytically predicted influence of the soliton velocity on its stability properties is verified numerically. We performed a set of simulations with the initial condition in a form of solitons with fixed value of λ and several values for the soliton velocity v. An example of these simulations is illustrated in Fig. 5. The standing soliton (v=0), with amplitude A_0=1.56, outside the stability region ($\lambda = 0.5$) relaxes toward corresponding stable soliton with the same photon number [Fig. 5(a)]. The moving soliton with the same λ but with the soliton velocity (v=0.3) slightly below the stability threshold exhibits a long-lived oscillations around the corresponding stable soliton state [Fig. 5(b)]. Further increase of the soliton velocity (v=0.7) turns the soliton inside the soliton stability region and the soliton propagation becomes stable [Fig 5(c)]. In this way we have confirmed our analytical prediction that the increasing soliton velocity shifts the instability threshold λ_s toward larger values and acts as a stabilizing factor.

For stable solitons being initially perturbed with the perturbations ε in a form of $\rho_p = \rho_0(1 + \varepsilon)$, internal oscillation modes are excited and solitons exhibit long lived oscillating behavior of the breather type. If the initial perturbation of the stable moving soliton grows, the frequency of the excited oscillations increases and amplitude excursion from the initial value grows. A further increase of the perturbation level leads to a further deviation from the stable state and eventually to a rapid aperiodic growth of the amplitude. In this stage, this process is very similar to the initial stage of the collapse phenomenon [4]. However, the amplitude growth is accompanied by a continuous change of the soliton profile toward a highly pointed structure of a cusp type. This process continues up to the point when the amplitude reaches the critical value $\rho_c \approx 1.55$, creating a highly unstable cusp structure. Creation of this structure coincides with a break up of the spectral numerical scheme (conservation loss for H and P) and it was not possible to follow the dynamic behaviour further. This is illustrated in Fig. 6, where the evolution of the initially launched moving (v=0.4) soliton with the photon number $P<P_{max}=P_0(\lambda_s)\approx4.45$, inside the stability region, for different level of the perturbations is followed.
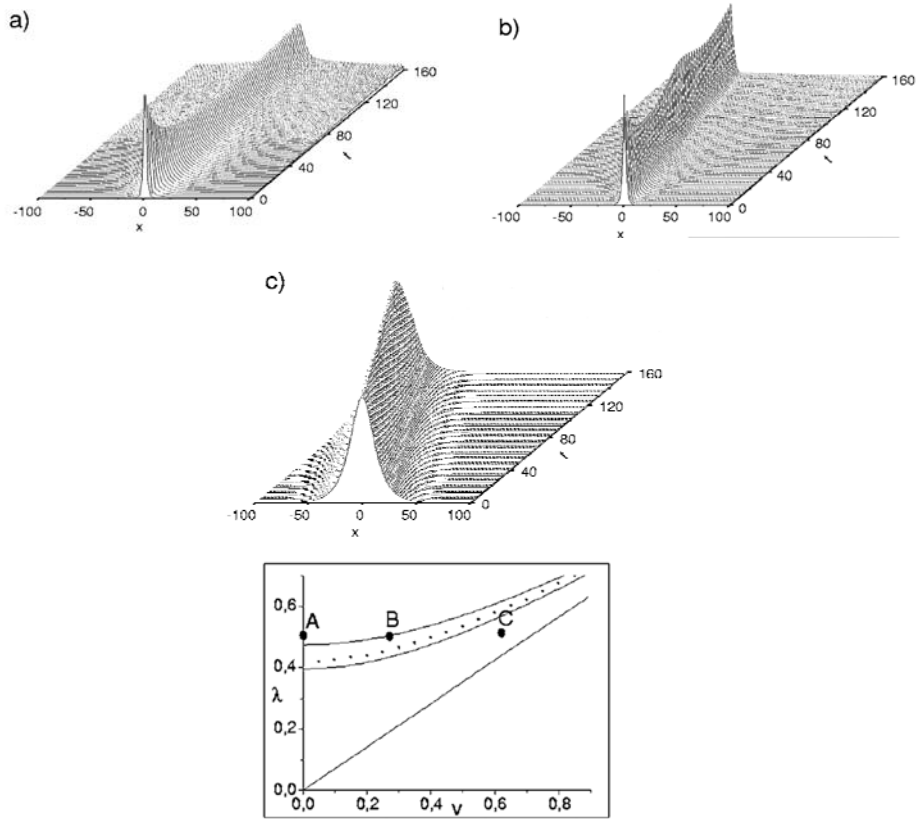
Fig. 5. Different dynamical regimes of the soliton with λ=0.5: a) Standing soliton in the unstable region with amplitude A_0=1.56, P=3.23; b) Moving soliton (v=0.3) in the unstable region, A_0=1.5, P=3.9; c) Moving soliton (v=0.7) in the stable region, A_0=0.26, P=1.34.

The observed long lived oscillations of the soliton amplitude show a similar behavior as in the case of the NLS equation with a local power-law nonlinearity, described in Ref. 24. This nonlinear evolution is illustrated in Fig. 7 in the $P_0(\lambda)$ diagram for the stable soliton $P_0 = 2.727, \lambda_0 = 0.334, v = 0.4$. The introduced perturbations (ε_1) at the stable soliton increase the photon number to $P_1 > P_0$ and excite internal oscillations around the new value of λ_1 which corresponds to the

111

stable soliton with P_1. During the oscillations, the soliton profile periodically changes its shape. Due to the influence of the nonlocal terms in Eq. (4), the periodic amplitude increase leads toward the cusp shape of the soliton profile. With the further perturbation increase (ε_2) the oscillatory behavior remains until the photon number reaches the value above $P_{\max}$ when the intersection with the curve $P_0(\lambda)$ is absent and the corresponding stable soliton solution cease to exist. In that case, a rapid aperiodic growth of the soliton amplitude creates a collapsing soliton structure up to the point when the amplitude reaches the critical value creating a cusp structure when we can no longer follow dynamic behaviour [25].

Initially launched stable moving solitons with parameters inside the stability region, but closer to the instability threshold, exhibit similar behavior, however, the level of the imposed perturbations that will lead to the soliton aperiodic growth, is much lower.
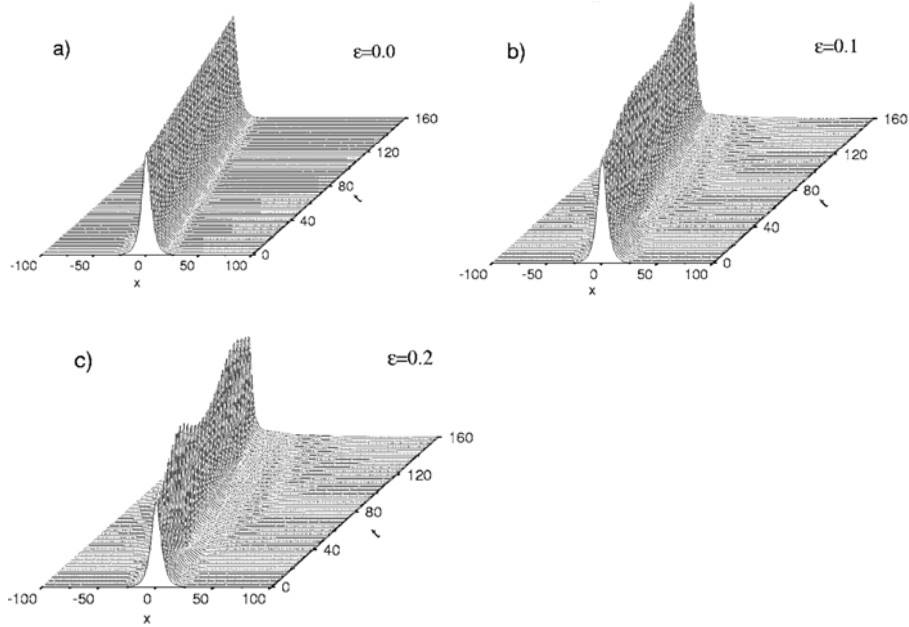
Fig. 6. Spatio-temporal evolution of initially launched moving soliton, in the stable region λ=0.334, v=0.4, A_0=0.6, P=2.73, for different perturbation levels.
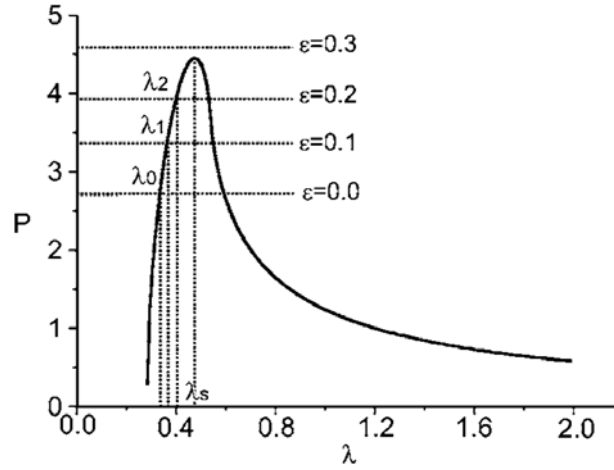
Fig. 7. Typical dependence of the photon number $P_0(\lambda)$ for solitons with v=0.4, P_{max}=4.45, λ_s=0.473. The stable soliton corresponds to the point P_0=2.727, λ_0=0.334. For the perturbation level ε_1=0.1 the photon number is P_1=3.3 and λ_1=0.36 of the corresponding stable soliton (amplitude oscillations around λ_1). For ε_2=0.2, P_2=3.927 and λ_2=0.39 of the corresponding stable soliton (amplitude oscillations around λ_2). For ε_3=0.3, the photon number is P_3=4.61> P_{max} and corresponding stable solution does not exist (soliton collapse-decay).

5. SOLITON INTERACTIONS

The type of soliton interaction depends on the parameters (amplitude, phase, velocity) of the colliding solitons. We restrict our study to symmetric collisions of two solitons with equal amplitudes and opposite velocities $v_1 = v, v_2 = -v$ [26]. Direct numerical simulations of the model equation (1) show that interaction of the small amplitude solitons is always elastic one (Fig. 8a), without energy (momentum) exchange between colliding solitons. By increasing the soliton amplitude, the interaction remains elastic up to the point when the resulting amplitude of the interacting soliton complex reaches the value of ρ_c and creates a highly unstable "cusp" -form structure. (Fig. 8b). Numerical simulations show a break up (annihilation) of the interacting pair. However, it is not possible to further follow chaotic dynamics due to the break up of the spectral numerical scheme (conservation loss for H and P). An introduction of the phase difference between the colliding soliton pair results in decreasing amplitude of the interacting complex and possible turn to the elastic type of interaction (Fig. 8c). Depending, whether during

113

impact, the soliton pair is in or out of phase, constructive or destructive interference of EM fields determines a fate of their interaction. Based on P-M-H interdependence future attempts to seek conservation laws for soliton interaction will be made.
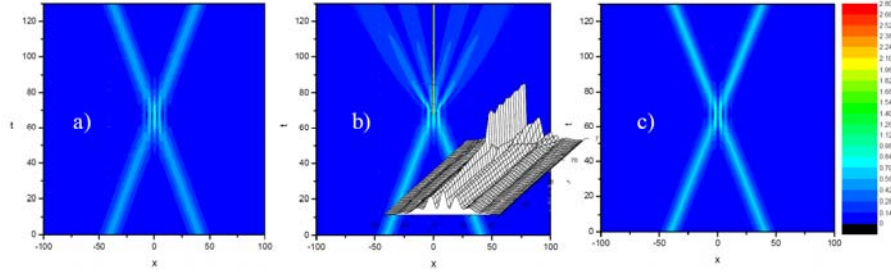
Fig.8. Interaction of two, in phase solitons with equal velocity v = 0:6 and different amplitudes a) $\rho_0 = 0.485$ and b) $\rho_0 = 0.6$ ½0 = 0:6, and c) solitons with same parameters as (b) with phase difference $\varphi = \pi$. The inserted plot illustrates the creation of the "cusp" structure.

VI. CONCLUSIONS

In this work, moving 1D electromagnetic solitons, formed in a weakly relativistic laser plasma interaction, were studied in the framework of the envelope GNLS equation (4). Moving EM soliton solutions and corresponding soliton photon number (*P*) and Hamiltonian (*H*) were analytically derived in a closed form. The stability analysis shows that the weakly relativistic moving EM solitons are stable; with the stability region shifting toward larger amplitudes in comparison to the standing soliton case. Numerical simulations of the model equation (4) have confirmed our analytical results. Moreover, further studies of the dynamics of the perturbed solitons, shows that the imposed perturbations excite internal oscillation modes leading to the creation of the breather type of structures. A further increase of the perturbation level leads to a further deviation from the stable state and eventually to a rapid aperiodic growth of the amplitude toward the critical amplitude ρ_c, accompanied by a continuous change of the soliton profile toward a highly pointed and unstable structure of a cusp type. Due to the coincidental break up of the model equation (4) and our numerical scheme, we were unable to follow the dynamics of this structure further. This question deserves future attention because our considerations were restricted to a weakly relativistic regime; therefore, the future studies of the obtained large relativistic EM structures are possible with fully nonlinear fluid-Maxwell [15] and particle simulations [27], which are beyond the scope of this work.

REFERENCES

1. A. I. Akkheizer and R. V. Polovin, Sov. Phys. JETP **3**, 696 (1956).
2. A. G. Litvak and A. M. Sergeev, JETP Lett. **27**, 517 (1978).
3. V. A. Kozlov, A. G. Litvak and E. V. Suvorov, Sov. Phys. JETP **49**, 75 (1979).
4. V. E. Zakharov, S. V. Manakov, S. P. Novikov, L. P. Pitaevski, *Theory of Solitons* (Plenum Press, New York, 1984).
5. K. V. Kotetishvili, P. Kaw, and N. L. Tsintzadze, Sov. J. Plasma Phys. **9**, 468 (1983).
6. M. Y. Yu, P. K. Shukla, and N. L. Tsintzadze, Phys. Fluids **25**, 1049 (1982).
7. S. V. Bulanov, I. N. Inovenkov, V. I. Kirsanov, N. M. Naumova, and A. S. Sakharov, Phys. Fluids B **4**, 1935 (1992).
8. P. K. Kaw, A. Sen, and T. Katsouleas, Phys. Rev. Lett. **68**, 3172 (1992).
9. T. Zh. Esirkepov, F. F. Kamenets, S. V. Bulanov, and N. M. Naumova, JETP Lett. **68**, 36 (1998).
10. D. Farina and S. V. Bulanov, Phys. Rev. Lett. **86**, 5289 (2001).
11. S. Poornokala, A. Das, A. Sen, and P. K. Kaw, Phys. Plasmas **9**, 1820 (2002).
12. M. Lontano, M. Passoni, and S. V. Bulanov, Phys. Plasmas **10**, 639 (2003).
13. K. Mima, M. S. Jovanović, Y. Sentoku, Z. M. Sheng, M. M. Škorić, and T. Sato, Phys. Plasmas **8**, 2349 (2001).
14. D. Farina and S. V. Bulanov, Plasma Phys. Control. Fusion **47**, A73 (2005).
15. V. I. Berezhiani, D. P. Garuchava, S. V. Mikeladze, K. I. Sigua, N. L. Tsintsadze, S. M. Mahajan, Y. Kishomoto, and K. Nishikawa, Phys. Plasmas **12**, 062308 (2005).
16. S. V. Bulanov, T. Zh. Esirkepov, N. M. Naumova, F. Pegoraro, and V. A. Vshivkov, Phys. Rev.Lett. **82**, 3440 (1999).
17. Y. Sentoku, T. Zh. Esirkepov, K. Mima, K. Nishihara, F. Califano, F. Pegoraro, H. Sakagami, Y. Kitagawa, N. M. Naumova, and S. V. Bulanov, Phys. Rev. Lett. **83**, 3434 (1999).
18. T. Zh. Esirkepov, S. V. Bulanov, K. Nishihara, and T. Tajima, Phys. Rev. Lett. **92**, 255001 (2004).
19. M. Tushentsov, A. Kim , F. Cattani , D. Anderson, and M. Lisak, Phys. Rev. Lett. **87**, 275002 (2001).
20. M. M. Škorić, Lj. Hadžievski, L. Baiwen, and S. Ishiguro, in *31st EPS Conference on Plasma Physics*, London, 28 June-2 July 2004, ECA (European Physical Society, Petit-Laney, 2004), Vol. 28G, O-2.10. J. Plasma Phys. (to be published)
21. Lj. Hadžievski, M. S. Jovanović, M. M. Škorić, and K. Mima, Phys. Plasmas **9**, 2569 (2002).

22. N. Akhmeidev and A. Ankiewicz, Phys. Rev. E. **59**, 6088 (1999).
23. T. R. Taha and M. J. Ablowitz, J. Comput. Phys. **55**, 203 (1984).
24. D. E. Pelinovsky, V. V. Afanasijev, and Y. S. Kivshar, Phys. Rev E **53**, 1940 (1996).
25. A. Mančić, Lj. Hadžievski and M.M.Škorić, Electromagnetic Solitons in Relativistic Plasmas, Phys. Plasmas, 13, 052309, (2006)
26. A. Mančić, Lj. Hadžievski and M.M.Škorić, Interaction of Electromagnetic Solitons in in Relativistic Plasmas, J. Plasma Phys. 72, 1309-1313 (2006)
27. L. Baiwen, S. Ishiguro, M. M. Škorić, M. Song, and T. Sato, Phys. Plasmas **12**, 103103 (2005).